An NMR view of the unfolding process of rusticyanin: Structural elements that maintain the architecture of a β-barrel metalloprotein

LUIS A. ALCARAZ,[1] BEATRIZ JIMÉNEZ,[2] JOSÉ MARÍA MORATAL,[3] AND ANTONIO DONAIRE[1]

[1]Instituto de Biología Molecular y Celular, Universidad Miguel Hernández, 03202-Elche (Alicante), Spain
[2]Center of Magnetic Resonance (CERM), University of Florence, 50019 Sesto Fiorentino (Florence), Italy
[3]Departamento de Química Inorgánica, Universitat de València, 46100 Burjassot (Valencia), Spain

(Received January 5, 2005; Final Revision March 29, 2005; Accepted April 8, 2005)

Abstract

The unfolding process of the blue copper protein rusticyanin (Rc) as well as its dynamic and D_2O/H_2O exchange properties in an incipient unfolded state have been studied by heteronuclear NMR spectroscopy. Titrations of apo, Cu(I), and Cu(II)Rc with guanidinium chloride (GdmCl) show that the copper ion stabilizes the folded species and remains bound in the completely unfolded state. The oxidized state of the copper ion is more efficient than the reduced form in this respect. The long loop of Rc (where the first ligand of the copper ion is located) is one of the most mobile domains of the protein. This region has no defined secondary structure elements and is prone to exchange its amide protons. In contrast, the last loop (including a short α-helix) and the last β-strand (where the other three ligands of the metal ion are located) form the most rigid domain of the protein. The results taken as a whole suggest that the first ligand detaches from the metal ion when the protein unfolds, while the other three ligands remain bound to it. The implications of these findings for the biological folding process of Rc are also discussed.

Keywords: rusticyanin; blue copper protein; NMR; protein unfolding; protein dynamics

Supplemental material: see www.proteinscience.org

The dynamics of the unfolded state in proteins and its comparison with that of the folded molecule can provide clues as to the structural elements essential in maintaining the three-dimensional conformation of a protein (Fersht and Daggett 2002; Ferguson and Fersht 2003; Vendruscolo et al. 2003). In turn, substantial thermodynamic information on the folding/unfolding process can also be obtained from these kinds of studies (Dinner et al. 2000; Daggett and Fersht 2003; Gianni et al. 2003). In this respect, NMR is one of the most widely used and thorough techniques. NMR is also a unique tool that allows characterization of the mobility features of each single amino acid in the unfolded state (Dyson and Wright 2002; Bruschweiler 2003; Jiménez et al. 2003b; Schwalbe 2003).

Metalloproteins, in general, and copper proteins, in particular, are stabilized to a large degree by the prosthetic group (i.e., the metal ion). In principle, this stabilizing effect occurs independently of the role of the metal ion in the function of the macromolecule. Blue copper proteins (BCPs) are relatively small, soluble electron transfer proteins (Malmström and Leckner 1998; Gray et al. 2000; Randall et al. 2000; Vila and Fernandez

Reprint requests to: Antonio Donaire, Instituto de Biología Molecular y Celular, Universidad Miguel Hernández, Edificio Torregaitán, Avda. de la Universidad s/n, 03202-Elche (Alicante), Spain; e-mail: adonaire@umh.es; fax: +34-96-6658758.

Abbreviations: Az, azurin; BCP, blue copper protein; GdmCl, guanidinium chloride; NMR, nuclear magnetic resonance; NOE, nuclear Overhauser effect; Rc, rusticyanin.

Article and publication are at http://www.proteinscience.org/cgi/doi/10.1110/ps.051337505.

 Copyright © 2005 The Protein Society

2001). They all possess a β-barrel structure and are arranged in a so-called Greek key topology, as shown in Figure 1. The redox potential of the copper ion is higher in BCPs than in aqueous solution, i.e., the reduced form is more stable than the oxidized species. BCPs are highly rigid. In fact, values of the generalized order parameter, S^2, obtained from NMR data, range from 0.83 to 0.93 (Kalverda et al. 1999; Thompson et al. 2000; Bertini et al. 2001a; Jiménez et al. 2003a). This rigidity is due to the large network of hydrogen bonds extending between the β-strands of these proteins, which in turn is necessary to fulfill their function (electron transport). The active site is particularly rigid. The copper ion is strongly bound to a sulfur atom of a cysteine ligand and to the imidazol nitrogen atoms of two histidine residues (HisN and HisC, respectively, according to their proximity in the sequence to the N- and C-terminal ends). In most of these proteins, an axial sulfur atom of a methionine, weakly bound to the metal, completes the pseudotetrahedral coordination (Randall et al. 2000) (see Fig. 1). This geometry, which remains essentially unaltered upon oxidation or reduction of the copper ion, is imposed by the protein scaffold. This is not the preferred coordination for the copper(II) ion and thus, the metal is found in a strained conformation (entatic/rack mechanism) (Malmström 1994). This characteristic permits a low reorganization energy, which is required for an efficient redox process (Gray et al. 2000; Crane et al. 2001). Traditionally, the strained coordination has also been related to the high redox potential of the BCPs (Malmström 1964, 1994). This concept was reviewed since the redox potential of the BCP Az is higher in the unfolded than in the folded state (Winkler et al. 1997; Wittung-Stafshede et al. 1998; Marks et al. 2004). Recently, an elegant theoretical study factorized the structural determinants of the relative redox potentials of the blue copper sites (Li et al. 2004). In this study, the investigators conclude that the entatic/rack mechanism is one of the major determinants of the relative redox potentials in BCPs. These findings lead us to consider the function of the metal ion in maintaining protein stability and, in turn, the role of protein folding in maintaining each oxidation state of the metal ion (i.e., in governing the redox potentials) in BCPs.

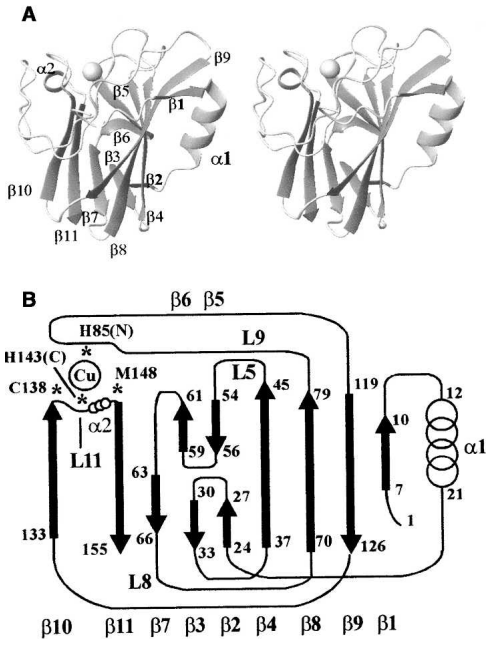

Figure 1. (*A*) Stereo view image of rusticyanin. Secondary structural elements are indicated. (*B*) Topology of the β-barrel Greek key of Rc. The β-strands are located according to the three-dimensional Rc structure (1cur file; Botuyan et al. 1996). The symbol * indicates the position of the ligands of the metal ion: HisN (His85 in Rc), HisC (His143 in Rc), Cys138, and Met148. The numeration of the β-strands is given at the *bottom* or at the *top* of the figure. The loops cited in the text are named with an upper-case L (the numeration of the loops is that of the following β-strand). Other numbers refer to amino acids indicating the beginning and the end of each β-strand.

Another important issue to address in the study of the metalloproteins is whether or not they take up the metal ion prior to their folding. Binding of copper (in whatever oxidation state) to the folded protein is presumably too slow to be biologically relevant (Pozdnyakova and Wittung-Stafshede 2001a; Wittung-Stafshede 2004). Consequently, the copper ion must bind to the BCP in the unfolded state, and is in fact known to do this (Leckner et al. 1997a,b; Pozdnyakova and Wittung-Stafshede 2001a; Marks et al. 2004). However, the oxidized state is not relevant in the cell since copper(II) is toxic (O'Halloran and Culotta 2000). As a result, copper must bind in its reduced form. Thus, it is biologically relevant to demonstrate the binding of copper(I) ion to the unfolded protein.

We have studied the role of the copper ion in the protein stability and dynamic features of Rc by means of NMR. Rc is unique among the BCPs. In fact, Rc possesses the highest redox potential of the BCP family, 680 mV (Nunzi et al. 1994). In other words, it is particularly efficient in stabilizing the copper(I) ion. Rc is also extremely stable at acidic pH values (<2.5) (Cox and Boxer 1978; Ingledew and Cobley 1980). The existence of a highly hydrophobic core in the molecule could explain, at least partially, these two singularities (Botuyan et al. 1996; Walter et al. 1996; Donaire et al. 2001). Nevertheless, the correlation between the structural and thermodynamic properties of Rc is not well understood and is still a matter of debate (Olsson et al. 2003; Li et al. 2004). To date, the role played by the metal ion and its oxidation state in maintaining protein stability is not well understood either. Hence, Rc represents an extremely interesting case in which to

identify the critical properties of BCPs that make these proteins especially efficient as electron mediators.

In this study we describe first, an NMR titration of apo, Cu(I), and Cu(II)Rc with guanidinium chloride (GdmCl); second, direct evidence of copper coordination (in both oxidation states) to Rc in its completely unfolded state; and third, a study of the dynamic and solvent exchange properties of the protein in an incipient or early step of the unfolding process. The former experiments help to interpret the role of the copper ion in maintaining the protein scaffold and the way in which the protein folds. The latter provide clues as to the secondary structural elements involved in starting the unfolding process. We recently described the formation of aggregated species in the unfolding process of Rc with GdmCl, using several biochemical and spectroscopic methods (Alcaraz and Donaire 2004). Here, the aggregation process is again evidenced. The present results have allowed us to identify the regions that are more resistant to the unfolding process and the structural features responsible for Rc stability.

Results

NMR titrations

Incipient unfolded state/fast exchange

The stability of Rc as a function of the guanidinium chloride concentration was monitored by heteronuclear NMR spectroscopy. Figure 2 shows the ^{1}H-^{15}N HSQC spectra of Cu(I)Rc at GdmCl concentrations of 0.0, 2.1, and 6.0 M. The addition of denaturant at low concentrations causes small changes in the ^{1}H and ^{15}N chemical shifts (in the fast exchange regime). This clearly indicates that the essential secondary and tertiary structural elements of the protein are maintained at this GdmCl concentration. In these conditions, the protein scaffold remains essentially unaltered as compared with the completely folded species. This represents a monomeric, essentially folded, species. It is essentially folded because its chemical shifts are substantially coincident with those of the completely folded Rc (see Fig. 2B). It is monomeric since the signals do not present line broadening. On the other hand, the completely unfolded species displays an HSQC spectrum typical of random coil proteins (Fig. 2C).

Figure 3, A–C, displays the differences in the ^{1}H and ^{15}N chemical shifts of the folded and incipient unfolded species for each HN pair in the reduced protein (the pattern is analogous for the apo and the oxidized forms; data not shown). The largest variations are observed in Gly28, in the middle (Ile89, Ile90, Asp103, and Val106), and at the end (Gly118) of the long loop L9 (the loop that links strands β8 and β9) (see Fig. 1); at

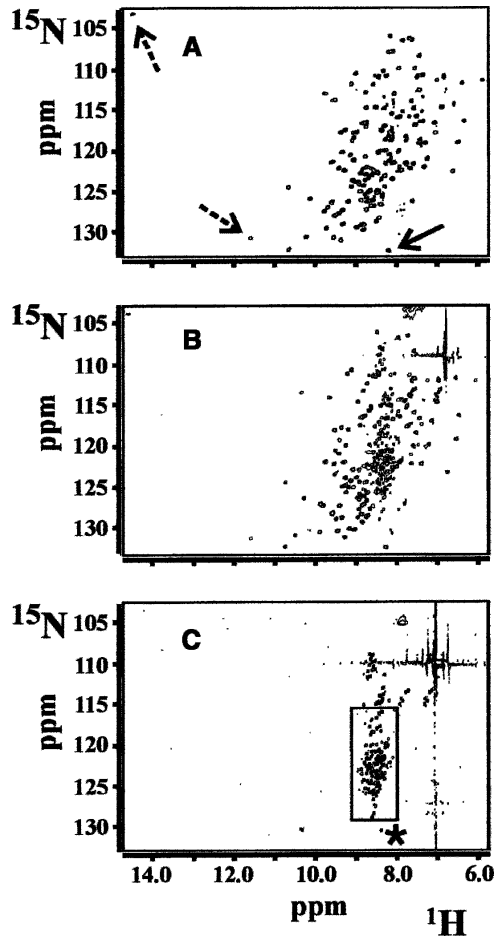

Figure 2. ^{1}H-^{15}N HSQC spectra of Cu(I)Rc at several GdmCl concentrations: 0.0 M (*A*), 2.1 M (*B*), and 6.0 M (*C*). The solid arrow in *A* indicates the signal corresponding to Ile155. Dotted arrows designate the signals corresponding to the imidazol protons of the two histidine ligands in the folded state (^{15}N chemical shifts of these two signals are 171.5 and 164.9 ppm for the signals at 14.5 and 11.5 ppm, respectively. They appear folded in the F1 dimension in the present spectra). The symbol * (*C*) specifies the signal of the completely unfolded species that serves as a reference for quantifying this species (see text; Fig. 4). The square in *C* displays the expanded region detailed in Figure 5.

the beginning of the β-strand β9 (Phe120, Gly121, Tyr122, and Thr123); and in some residues of the β-strand β8 (Val74, Thr75, and Phe76). Thus, these three secondary structural elements (β-strands β8 and β9, and the long loop L9) have a manifest tendency to change when the protein starts to open. It is remarkable that both strands, β8 and β9, face each other in the three-dimensional structure of Rc (see Fig. 1). Other groups that experience changes are those belonging to the end of the strand β4 (Ala42, Ala43, and Leu46). Another three residues (Asp58, His128, and Thr130) also experience observable changes in their chemical shifts. They are close (sequentially and spatially) to the

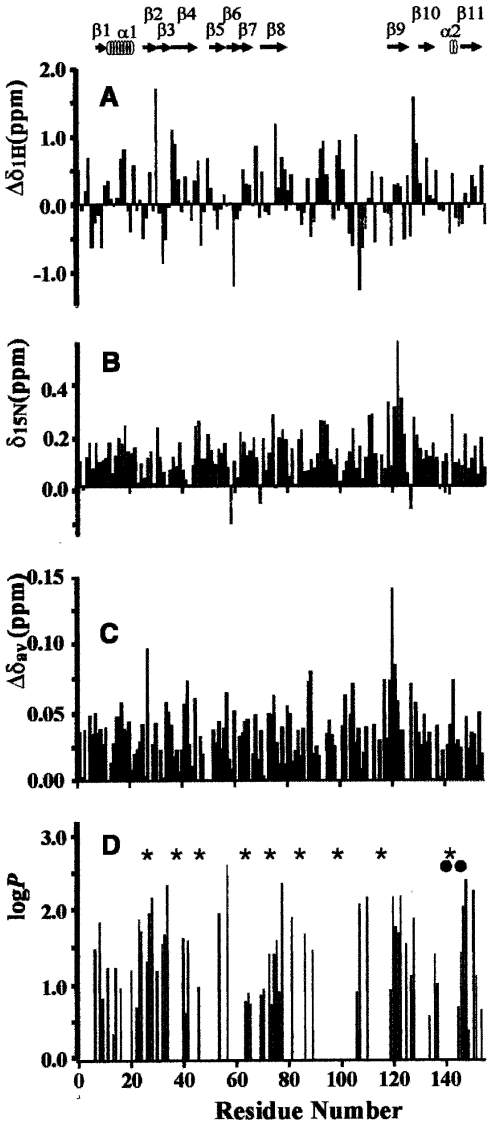

Figure 3. Differences between the completely folded and incipient unfolded species in Cu(I)Rc (i.e., species found at 2.1 M GdmCl): ^{1}H chemical shifts (*A*); ^{15}N chemical shifts (*B*); weighted average values (*C*) ($\Delta\delta_{av}$) according to Equation 1. (*D*) Logarithm of the protection factors of the amide protons in the incipient unfolded state of Rc. The secondary structural elements are plotted at the *top* of the figure. The symbols * and • display the position of the amide protons that give cross peaks in the cleanex and the ePHOGSY experiments, respectively (see Supplemental Material).

two free (nonligand) histidines of the protein (His57 and His128). The changes in their chemical shifts are probably related to protonation–deprotonation phenomena of both histidines at the working pH value.

Most of these HN pairs form hydrogen bonds with carbonyl groups, and are essential in keeping the β-barrel structure. Moreover, most of them increase the chemical shifts of their amide protons, indicating an increment in the strength of the hydrogen bonds. Only four of these amide protons (Gly28, Asp103, Gly118, and Gly121) are exposed to the solvent and do not form hydrogen bonds. These changes may be due to direct interactions with molecules of the denaturant agent.

Unfolded protein/slow exchange

Subsequent increments in the denaturant agent concentration produce substantial changes in the intensity of the peaks observed and, at a particular concentration of GdmCl (depending on the form studied), a new set of signals starts to appear in slow exchange regime. As observed in Figure 2C, the low spread of ^{1}H and ^{15}N chemical shifts in the last set of signals (at GdmCl 6.0 M) clearly corresponds to an unfolded species. Complete extinction of the folded species is reached at this GdmCl concentration for Cu(I)Rc. For the other two forms, apo and Cu(II)Rc, essentially the same phenomena are observed, although they occur at different concentrations of the denaturant agent.

Figure 4 (symbol ○) shows the molar fraction of the peak corresponding to the well-resolved signal of Ile155

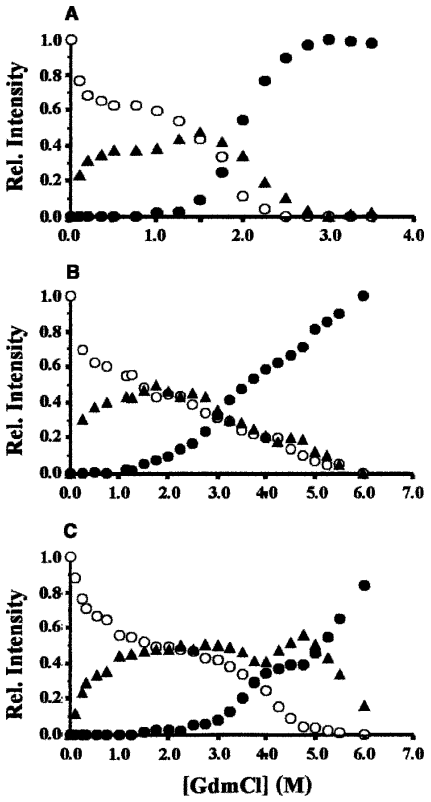

Figure 4. NMR titrations of Rc with GdmCl for the apo (*A*), reduced (*B*), and oxidized (*C*) forms. For the folded species (○), the volume of the Ile155 signal (dark arrow in Fig. 2A) was measured. For the unfolded species (•), the volume of the resolved signal indicated by the symbol * in Figure 2C was recorded. The molar fractions of the aggregated species (▲) were calculated from Equation 2 (see Discussion).

(see Fig. 2A) as a function of the GdmCl concentration for the apo (Fig. 4A), reduced (Fig. 4B), and oxidized (Fig. 4C) protein. Another 20 well-resolved HN pairs distributed throughout the protein were analyzed and very similar results obtained (data not shown). Thus, this process takes place at the same time throughout the molecule. Three regions can be discerned in each of these curves. First, the peak volumes drastically decrease (until they reach ~55%–60% of the original volume) as the GdmCl concentration increases from 0 to 0.7 M. This last concentration is independent of the form of Rc considered. This decrease is not accompanied by the appearance of any new set of signals. Therefore, it must be related to the formation of a "silent" species (from the NMR point of view). By means of gel filtration and cross-linking experiments, we recently showed that aggregated species are formed when GdmCl is added to Rc (Alcaraz and Donaire 2004). The loss of intensity observed here is related to the presence of these aggregated species, whose proton signals are too broad to be detected. Second, a less pronounced (almost flat) decrease in the peak volumes is observed for GdmCl concentrations between 0.7 and 1.0 M for the apo form; 0.7 and 1.7 M for the reduced form; and 0.7 and 2.2 M for the oxidized form. Finally, a sigmoid-like behavior is observed in the last part of each curve. Signals corresponding to the incipient unfolded species completely disappear at GdmCl concentrations of 2.5 M for apoRc and 5.5 M for both holoproteins (Fig. 4, symbol ○). The midpoints for the sigmoid curves are 1.7 (apoRc), 3.0 (reduced Rc), and 4.0 M (oxidized Rc). The present data clearly indicate that the folded apoRc is less stable (compared with the unfolded species) than both forms of the holoprotein. In turn, Cu(II) is more efficient than Cu(I) in stabilizing the folded state. The same stabilizing effect of the metal ion has been observed in azurin (Leckner et al. 1997a,b; Marks et al. 2004).

In Figure 4 the normalized intensity of a well-resolved signal in the unfolded state (peak labeled with the symbol * in Fig. 2C) is also shown (symbol •). All the analyzed signals belonging to the unfolded species behave in a similar way. For the three forms of Rc (apo, reduced, and oxidized), these peaks start to appear at GdmCl concentrations of ~1.3 M, although the pattern of the volumes differs depending on the concentration of GdmCl. For the apoRc (Fig. 4A), a well-delineated sigmoid is observed with the midpoint at 2.0 M, and titration is complete at 2.8 M. In the case of Cu(I)Rc, an ill-defined step is observed (Fig. 4B), and titration is complete at 6.0 M. For the oxidized form (Fig. 4C), titration is almost, but not quite, complete at the last point (higher GdmCl concentrations could not be reached because dilution of the protein prevented HSQC spectra from being obtained). It may be deduced from this figure that there are two steps in this titration: The first step is due to the formation of aggregated species and the second to the unfolding process itself. Probably the same situation is found in the Cu(I)Rc unfolding process (Fig. 4B), although here both processes overlap (and this is why the ill-defined step is observed) (see above). However, in the oxidized state the situation is even more complicated since it is well known that the copper(II) ion reacts slowly with the thiol atom of the cysteine ligand in inorganic complexes or in the unfolded form of Cu(II)Az (Leckner et al. 1997a; Winkler et al. 1997). An analogous reaction could take place in the Rc unfolding process at the final points of the titrations. This slow process could affect the measurement of the two final points of the Cu(II)Rc titration (at very high GdmCl concentrations). Due to the presence of different species (aggregates) in solution, the interpretation of these data in a quantitative way (i.e., to extract thermodynamic data) is not straightforward at this stage and these data can only be analyzed in a qualitative way.

Final points for the apo and holoproteins

The final points for apo, Cu(I), and Cu(II)Rc are shown in Figure 5. The three spectra are superimposable, although a few peaks (labeled with * in Fig. 5B) show a very small intensity in the Cu(II)Rc spectrum or even disappear (signals labeled with lowercase letters). This indicates that the copper(II) ion is bound in the unfolded state. In fact, the signals belonging to the protons close to the metal ion decrease their intensity due to the paramagnetic effect (Bertini et al. 2001b; Donaire et al. 2002). Further evidence of copper(II) coordination in the unfolded state is given by the 1D ^{1}H superweft spectrum of the oxidized Rc in these conditions (Fig. 5C). The two broad signals observed at −22.5 (signal e) and −75 ppm (signal f) can only derive from protons with contact contribution to their isotropic shifts; i.e., they belong to ligands of amino acids covalently bound to the copper(II) ion (Donaire et al. 2002). Coordination of the reduced copper ion is also supported by comparison of the three HSQC spectra. In fact, the signals that disappear in the Cu(II)Rc spectrum (signals a–d in Fig. 5B) are the ones that change their position from the apo to the Cu(I)Rc spectrum (Fig. 5A). This strongly suggests that the copper(I) ion is also bound in the completely unfolded species.

Further evidence of copper coordination in the unfolded species is supported by atomic absorption spectroscopy. In fact, according to these data, 95 ± 2% of unfolded Rc retains copper(I) after three washes by dialysis. Copper(II) is also retained in a similar percentage (93 ± 2%) in the unfolded protein.

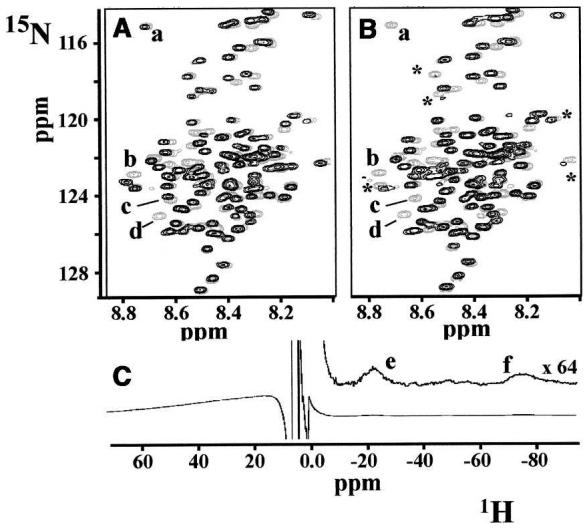

Figure 5. Final NMR spectra of Rc titrations with GdmCl. (*A*) Superposition of the ^{1}H-^{15}N HSQC spectra of apo and Cu(I)Rc. (*B*) Superposition of the ^{1}H-^{15}N HSQC spectra of Cu(II) and Cu(I)Rc. In both panels, the spectrum corresponding to the reduced species is drawn in light gray, while the apo (*A*) and the oxidized (*B*) spectrum are colored in black. The signals labeled a–d disappear in the Cu(II)Rc spectrum. The signals labeled with * (*B*) decrease their intensity in the Cu(II)Rc spectrum. *C* displays the ^{1}H superweft spectrum of Cu(II)Rc in the completely unfolded state. The upfield region of this spectrum is vertically expanded to observe signals e and f, hyperfine shifted. For the three spectra, the sample conditions were GdmCl 6.0 M, acetate buffer 10 mM (pH 5.5) (296K).

Solvent accessibility in the incipient unfolded species

A lyophilized Cu(I)Rc sample was dissolved in D_2O in the presence of 2.1 M GdmCl, and then, a set of ^{1}H-^{15}N HSQC experiments were performed consecutively. One hundred and three peaks corresponding to the incipient unfolded species were observed in the first experiment. Figure 3D displays the protection factors of these amide protons. Most of the HN protons with low protection factors belong to loop regions (including the long loop L9). Regarding the secondary structural elements, the β-strands β6 and β10 have a small tendency to exchange their amide protons with the solvent and strands β5 and β7, a moderate tendency, while the most protected protons belong to the rest of the β-strands.

It is interesting to note that all the residues belonging to the last β-strand as well as those from the short α-helix α2 (both structures are close to the metal ion and contain the last three ligands of the metal) posses amide protons with medium or elevated protection factors. Thus, the hydrogen bonds of these amino acids are relatively hidden from the solvent; i.e., these two structures are highly robust in this early step of denaturation.

In the same Figure 3D the results of the cleanex (Hwang et al. 1998) and the ePHOGSY (Dalvit and Hommel 1995; Dalvit 1996; Bertini et al. 1997) experiments performed in a reduced sample at 2.1 M GdmCl are also shown. The cleanex experiment (Supplemental Material) essentially displays the same cross peaks as those previously found for the native protein (Jiménez et al. 2003a). The most remarkable feature of this spectrum is the three strong cross peaks corresponding to the amide protons of Ser34 and Gly28 (found in loops L3 and L4, respectively) and to the His143 Hδ1 proton.

Peaks observed in the ePHOGSY experiment (Supplemental Material) (Dalvit and Hommel 1995; Dalvit 1996) may arise from a direct NOE between protein groups and a water molecule "trapped" within the protein frame. However, as already described, other effects may contribute to ePHOGSY peaks in the absence of a real HN-water NOE (Bertini et al. 1997). These are spin diffusion effects during the mixing time, the unwanted NOEs arising from Hα protons with the same chemical shifts of bulk water, and exchanged relayed NOEs. When all these effects have been properly taken into account, only the Gly142 and the Val145 amide protons unambiguously arise from direct HN–water NOEs. When we inspect the Rc crystallographic structure, 1rcy file (Walter et al. 1996), only the water molecule numbered 212 forms a hydrogen bond with the amide protons of these two amino acids, as well as with the carbonyl oxygen of Val98. Therefore, this structural water molecule (that is still present in the incipient unfolded state) links with the loop L11 and the beginning of the helix α2 on one side, and with the loop L9 on the other (see Fig. 1).

Mobility studies

Mobility studies of the protein backbone in the incipient unfolded state (GdmCl 2.1M) were performed (see Fig. 2B). Measurements of the ^{15}N relaxation rates and ^{1}H-^{15}N NOE values were carried out in a reduced Rc sample. Figure 6 shows the experimental data. The relaxation values of 100 of the 140 HN pairs of this protein (Rc possesses 155 amino acids, 14 of which are proline residues) were analyzed. Average values for the longitudinal and transversal relaxation rates (eliminating mobile residues as indicated in Materials and Methods) were 1.6 ± 0.2 and 10.5 ± 1.5 sec^{-1}, respectively (R_2/R_1 ratio of 6.5 ± 1.7 sec^{-1}). The average value of the ^{1}H-^{15}N NOEs was 0.74 ± 0.14. The signals belonging to the residues Thr2, Leu3, Ala44, Thr79, and Gly108 showed R_1 values significantly lower than the average (Fig. 6A). The residues Thr2, Leu3, Thr11, Lys36, Gly69, Thr79, Ala97, and Gly108 displayed low R_2 values (Fig. 6B). Of these, residues Thr2, Leu3, Thr79, and Gly108 also gave negative NOE values (Fig. 6C). These regions experience motions on the pico- to nanosecond timescale. On the contrary, the residues His57, Asp58, Leu64, Glu65,

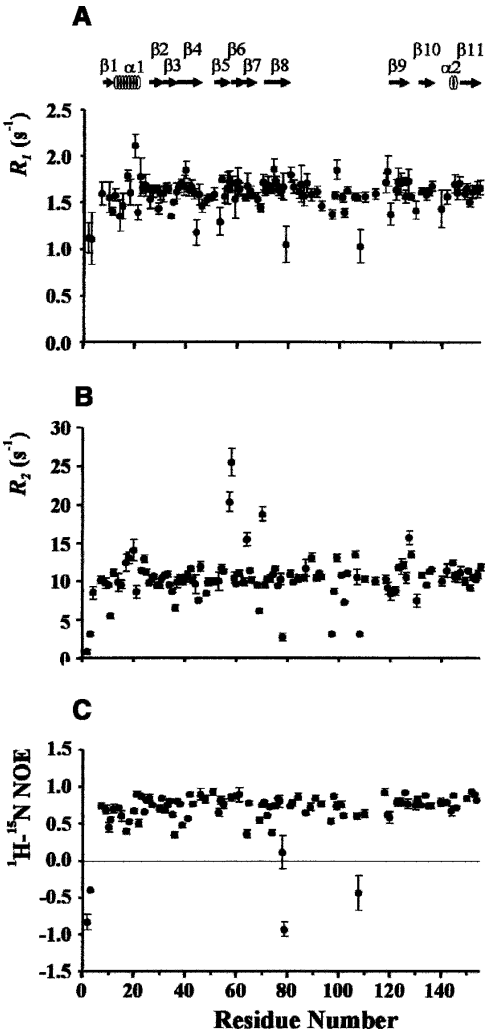

Figure 6. Relaxation data of the incipient unfolded species of Cu(I)Rc: longitudinal relaxation rates (*A*), transversal relaxation rates(*B*), and heteronuclear ^{1}H-^{15}N NOE data (*C*). The position of the secondary structure elements of Rc are shown at the *top* of the figure. Sample conditions: GdmCl 2.1 M, acetate buffer 10 mM (pH 5.5).

Ala70, and Trp127 displayed R_2 values higher than the average value (Fig. 6B); i.e., they experience conformational exchange on the micro- to millisecond timescale. His57 has been shown to undergo a protonation/deprotonation process at the working pH value in the folded state (Jiménez et al. 2003a). Leu64 and Glu65 belong to the short β-strand β7, while Ala70 is located on the short loop L8 (connecting strands β7 and β8) (see Fig. 1). Consequently, the β-strand β7 is one of the domains with a propensity to change to an open conformation.

Model-free analysis

The inertia tensor calculated from the R_2/R_1 ratios gave a value of 9.0 nsec for the correlation time of Rc at GdmCl 2.1 M. This value is similar to that previously reported for the protein in the native state, 9.6 nsec (Jiménez et al. 2004). Likewise, this value corresponds to that expected for a monomer species with such a molecular weight (Campos-Olivas and Summers 1999; Banci et al. 2000). Hence, the results presented here correspond to a monomer species. This value indicates that other possible species present in solution (aggregates and unfolded species) (see Discussion) are in a slow exchange regime.

The relaxation parameters were fitted to the dynamic isotropic model (Mandel et al. 1995). No statistical improvement was observed when more independent variables were added (axially symmetric and totally anisotropic models). Once the isotropic model for the global protein was assumed, the relaxation data for each individual HN peak were fitted to the five models previously described (Mandel et al. 1995). The values of the generalized order parameter (S^2) per residue are shown in Figure 7A. The average value (discarding those whose standard deviation was $>2\sigma$) was 0.83 ± 0.07, slightly but significantly slower than that reported by us for the native protein, 0.93 ± 0.03 (Jiménez et al. 2004). Fifty-seven of the 100 residues were fitted according to model 1 and 28 were fitted to model 2 (i.e., they present

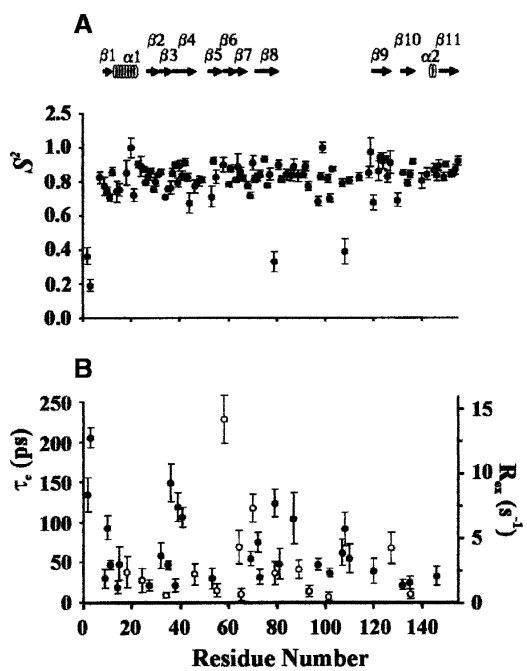

Figure 7. Results of the model-free analysis. (*A*) Generalized order parameter, S^2, vs. the residue number for the reduced Rc. (*B*) Correlation times (τ_e, filled dots, *left Y*-axis) for residues with fast (subnanoseconds) internal motions (these residues were fitted according to models 2 or 4) and exchange rates (R_{ex}, open dots, *right Y*-axis) for residues implicated in dynamics in the micro- or millisecond timescale (models 3 or 4).

mobility on the subnanosecond timescale). Thirteen residues presented conformational exchange (they belong to model 3) and two of them (Thr79 and Tyr135) experienced both kinds of motions (model 4). Figure 7B displays the values of the correlation times of the internal motions, τ_e, and the exchange rates, R_{ex}, for these residues (Mandel et al. 1995).

Three regions of the protein (the N-terminal end, and the residues close to Thr79 and Gly108) are highly disordered (see Fig. 7A), with values of $S^2 < 0.4$. It is interesting to note that Thr79 is at the beginning of the long loop L9 (see Fig. 1), which lacks a defined secondary structure. It is also noticeable that His85, the first ligand of the copper ion in the sequence, is sequentially and spatially close to this region. Ala97 and Ile102 (Fig. 7A) are another two amino acids with small order parameters (0.68 and 0.70, respectively), while Val101 experiences conformational exchange (see Fig. 7B). All these residues belong to the same long loop L9 and are close to a region rich in proline residues (residues 94, 95, 100, and 104 are prolines). These data taken as a whole indicate that the surroundings of this region have a propensity to experience mobility on a large range of timescales (some on the pico- or nanosecond timescale, others on the micro- to millisecond timescale) (see Fig. 7B). Taking into account the fast exchange properties of the loop L9 (see Fig. 3D), we conclude that (excluding the N-terminal end) the region rich in proline residues is the most flexible region of the protein.

Other residues with S^2 values lower than the average are Ala44, Leu46, and Phe51 (Fig. 7A). They are either at the end of the β-strand β4 or on the following loop (L5). These are two secondary structural elements with HN protons that exchange easily (see Fig. 3D). This loop contains three prolines (amino acid numbers 47, 50, and 52) and a glycine (Gly48), which are typical residues with a predisposition to undergo conformational movements. Finally, Thr130 also displays a generalized order parameter (0.69) lower than the average, which could be related to the protonation/deprotonation equilibrium of the nearby His128.

Discussion

Rc species present in the unfolding process

Our present NMR data clearly indicate the existence of three different forms of rusticyanin when the unfolding process takes place. At low concentration of the denaturant agent, the folded species starts to change slightly, in a fast exchange regime, toward a more open conformation. This form retains essentially the same secondary and tertiary structural elements as the folded form. This species represents the first stage of the denaturation process. We previously showed that this species has a hydrodynamic radius greater than that of the folded protein (Alcaraz and Donaire 2004), so we define this new species as an incipient unfolded (essentially folded) state.

When GdmCl is added to a solution containing Rc, the first observation is a drastic decrease in the volume of the peaks (see Fig. 4A–C). Integrals of these volumes (corrected by the dilution factors) are very different from those of the initial signals. Thus, nondetected species (i.e., with fast transversal relaxation rates) must be responsible for the percentage of the signal lost. By means of gel filtration chromatography and glutaraldehyde cross-linking experiments, we previously demonstrated the existence of aggregated species in Rc when GdmCl is present (Alcaraz and Donaire 2004). We conclude that these aggregates are present in solution in our NMR titrations. It should be pointed out that these aggregates are in a slow regime exchange with other species, since no changes either in the line broadening or in the relaxation properties of the signals are observed. This suggests that such an aggregation process, affecting the molecule as a whole, must be relatively slow on the NMR timescale. In turn, these aggregates must be made up of at least four monomers per molecule (since simpler structures would be observed). Taking into account these considerations, expression 2 (see Materials and Methods) is sufficiently justified. From this equation, the molar fraction of all species (including aggregated species) can be deduced. In Figure 4, the percentages of the aggregated species are also displayed.

The unfolding processes of other BCPs have been studied (Leckner et al. 1997b; Capaldi et al. 1999; Bai et al. 2001; Mizuguchi et al. 2003; Pozdnyakova and Wittung-Stafshede 2003; Sandberg et al. 2003) and no aggregation forms were found. Nevertheless, it is well known that similar aggregates have been identified in β-barrel proteins (Kobayashi et al. 2000; Kjellsson et al. 2003). The presence of these states in Rc is probably related either to the high content in hydrophobic residues of this BCP or to the fact that this is the largest BCP. Indeed, the protein size is a crucial parameter to discern between proteins that unfold in a two-step process from those that unfold via intermediates (Dobson 2003).

Hints from the unfolding process

Figure 8 classifies the secondary structural elements of Rc according to the parameters derived from our NMR experiments. High *P*-factors and high S^2 values indicate residues hidden from the solvent and/or belonging to

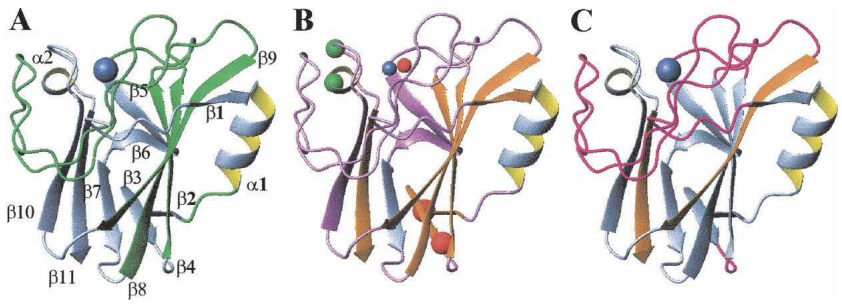

Figure 8. Schematic classification of the structural elements of Cu(I)Rc according to the NMR properties of the amide protons in the incipient unfolded state (GdmCl 2.1 M). (*A*) Average weighted chemical shifts. The secondary structural elements with the largest deviations in their amide chemical shifts are drawn in green. (*B*) *P*-factors. Secondary structural elements with low and high *P*-factors are colored in light purple and orange, respectively. Red and green circles indicate the positions of the NH pairs obtained from the cleanex and the ePHOGSY experiments, respectively. (*C*) Generalized order parameter, S^2. The β-strands β9 and β11, with S^2 values higher than the average are colored in orange. The domains with low S^2 values are colored in light purple. The copper atom is colored in blue.

highly rigid substructures of the protein. In contrast, low protection factors and low generalized order parameters, as well as the existence of cleanex cross peaks, designate the regions exposed to the solvent and lacking a robust structure. The information that the variations in the chemical shifts provides is more ambiguous. Large differences in this parameter derive from chemical changes in the surroundings of the amide protons. On the one hand, amide protons exposed to the solvent (such as those belonging to loop regions or to glycine residues) can modify their chemical shifts simply because of the change in the solvent polarity when passing from water to GdmCl. This would be the case of the amino acids close to the regions rich in proline residues (loops L5 and L9). On the other hand, amide protons belonging to the strands β5, β8, and β9 (see Fig. 8) probably increase the strength of the hydrogen bonds in which they participate. In effect, the average chemical shift variations found here are due, in most cases, to an increment toward the downfield regions of the proton chemical shifts. Then, these chemical shift variations reflect β-strands that interact more strongly with each other when the protein starts to unfold. In turn, the large mobility that the loops L5 and especially L9 experience in the incipient unfolded state probably permits the interaction between these three chains to increase.

All these data taken as a whole (Fig. 8) unequivocally indicate that two domains are the first to undergo the unfolding processes: the N-terminal end and the loop L9 (mainly in the region rich in prolines). Another two regions have a similar, although not so pronounced, behavior: On the one hand, the loop L5, which also possesses a large degree of mobility on the pico- to nanosecond timescale (see Fig. 7B); and, on the other hand, the loop L8, close to Ala70, which experiences mobility on the micro- to millisecond timescale (see Fig. 7B).

In contrast to these mobile, accessible regions, the most rigid, buried structures of the protein correspond to the β-strands (especially β-strands β9 and β11) and to the short α-helix α2. Two of the ligands of the metal ion (His143 and Met148) are located in these secondary structural elements. This means that the metal ion interactions are essential in maintaining this structure (as is also deduced from the corresponding titrations) (see Fig. 4).

Role of the copper ion

NMR titrations unequivocally demonstrate the stabilizing effect of the metal ion in Rc unfolding. Formation of the completely unfolded state is dependent on the metal ion and its oxidation state (see Fig. 4A–C). This confirms that not only the global tertiary conformation of the protein but also the metal ion architecture itself is modified in this step. In the case of the apo form, complete formation of the unfolded species is reached at 2.8 M GdmCl (see Fig. 4A), while a 6.0 M concentration is necessary to obtain the same result for Cu(I)Rc. With the oxidized protein, some nonnegligible aggregation exists (Fig. 4C), even at the last point of the titration (6.0 M). The midpoints of the titrations follow the order Cu(II) > Cu(I) > apo (Fig. 4, symbol •). Consequently, the same order is maintained for the stabilizing effect in the folded as compared with the unfolded forms. In other words, the copper ion provides Rc with an excess of thermodynamic stability compared with the apo form. In this respect, the oxidized state seems to be more effective than the reduced one.

The stabilizing effect of the metal ion is also corroborated by the fact that the domain containing the metal ion (i.e., the α-helix α2 and the strands β10 and β11) is one of the most rigid regions of the protein. Also, the

hydrogen bonds in this domain present slow exchange. Therefore, these secondary structural elements are strongly bound to each other.

The thermodynamic cycles of the unfolding process for the apo, Cu(I), and Cu(II) forms of Az have been studied in detail (Marks et al. 2004; Wittung-Stafshede 2004). In Az, copper(II) stabilizes the folded form more efficiently than the reduced species does. At first glance, this result seems contradictory to the fact that the azurin redox potential is higher than that of the Cu(II)/Cu(I) pair in aqueous solution; i.e., the reduced state is stabilized to a greater extent than the oxidized state in the folded form (Vila and Fernandez 2001). The apparent paradox vanishes if we take into account that the reduced and the oxidized forms of the completely unfolded conformations of Az are different (Pozdnyakova et al. 2001; Marks et al. 2004), so no direct comparison between the two unfolded titrations can be made (both their starting and final points are different). Our present results for Rc are analogous to those obtained for Az.

In the oxidized form of the unfolded Az, it is known that the copper ion is coordinated to a cysteine, a methionine, and a histidine ligand (HisC) (Pozdnyakova et al. 2001; Marks et al. 2004). These three ligands are on the same loop of the metal ion for all the BCPs (Buning et al. 2000; Donaire et al. 2002) (see Fig. 1). Figure 5 clearly shows that the copper ion (in both oxidation states) is coordinated to the unfolded Rc. From these spectra it is not possible to make deductions concerning ligands of the metal ion. However, other data here reported provide us with clues to the identity of such possible ligands. In fact, the last loop and the last β-strand are precisely the least disordered regions of Rc in the incipient unfolded state (Fig. 7). Moreover, their amide protons exchange very slowly with the solvent (Fig. 8B). These two data taken together indicate that this is the most rigid domain of the protein. In turn, since the distinctive feature of this region is its coordination to the metal ion, and since the metal ion clearly maintains the stability of the protein (see Fig. 8), we suggest that these three amino acids (Cys138, His143, and Met148) are probably coordinated to the metal ion in the unfolded state of Rc.

It has been shown that HisN is not coordinated to the metal ion in the unfolded state of Az (Romero et al. 1998; Pozdnyakova et al. 2001). HisN in Rc, as in all BCPs (Buning et al. 2000), is located in another domain of the protein (see Fig. 1). Our relaxation data show that the domain where this ligand is located (the loop L9) is one of the most mobile regions of the protein. It is thus likely that this histidine is not coordinated to the metal ion in the completely unfolded form; i.e., Rc shows the same pattern as that observed in Az (Romero et al. 1998; Pozdnyakova et al. 2001). Moreover, the equivalent region to this long loop in the folded forms of Az (Kalverda et al. 1999), pseudoazurin (Thompson et al. 2000) and plastocyanin (Bertini et al. 2001a) also present a relatively high degree of mobility. Then this could be a general process in BCPs: The ligands close together in the amino acid sequence (HisC, and the cysteine and methionine residues, all sited on the last loop) remain bound to the metal ion when the protein unfolds, while the ligand far from the others in the primary structure (HisN) (see Fig. 1) disrupts its interaction in the unfolding process.

Relevance in the biological folding process

Two features can be deduced from the mechanism of Rc folding. The first is related to the role of the proline regions. The two most mobile regions of Rc (L5 and L9) posses a high content of proline residues. The correct *cis–trans* conformations of proline residues are decisive in the speed of the folding of the BCP plastocyanin (Dyson et al. 1992; Bai et al. 2001). In fact, an erroneous conformation of the proline residues gives rise to non-active structures in the protein folding process. The high flexibility of the proline regions in Rc results in a low energy barrier to correct bad conformations if such misfolding processes occur.

The second characteristic relates to the kinetics of the process and the uptake of the metal ion by the protein. In the case of the BCP Az, the speed of formation of the three-dimensional protein structure is dependent on the tertiary contacts of the β-barrel (Pozdnyakova and Wittung-Stafshede 2002, 2003). It is also independent of the metal ion (Pozdnyakova and Wittung-Stafshede 2001b). However, formation of the active protein (the holoprotein) is closely related to the sequence of necessary events (protein folding and copper uptake). While in the case of Az, the binding of the copper is fast (of the order of milliseconds) for the unfolded protein, it is quite slow (from minutes to hours) for the folded protein (Pozdnyakova and Wittung-Stafshede 2001b). We obtained similar results with Rc by stopped-flow measurements (L. Alcaraz and A. Donaire, unpubl.). Thus, it was concluded that the copper ion bound to the protein prior to its folding (Wittung-Stafshede 2004). With our present data we can conclude that a similar behavior is likely to happen with Cu(II)Rc.

A doubt remains about the oxidation state of the copper ion in this process. In fact, in Az most of the evidence of copper coordination is related to the oxidized state. Nevertheless, copper(II) is toxic in the cell, and only the reduced form is found (O'Halloran and Culotta 2000). Our data (Fig. 5B) indicate that copper(I) is also bound in the unfolded state of Rc, thus making the mechanism proposed above possible.

Materials and methods

Sample preparation

^{15}N-labeled rusticyanin was obtained from BL21(DE3) *Escherichia coli* containing the Rc plasmid (Hall et al. 1996). The bacteria cultures were performed in M9 media adequately modified (Jiménez et al. 2003a). The samples (apo, reduced, and oxidized Rc) were prepared as previously described (Jiménez et al. 2003a). The metallation of the apoprotein was achieved by adding the metal ion in a 1:1 apoprotein:copper molar ratio. The samples were incubated with ethylenedyaminetetraacetic acid (EDTA) for 1 h and dialyzed several times against buffer to eliminate any possible excess of the chelating agent. All samples contained 8% D_2O for the lock signal. The conditions for all experiments were acetate buffer 10 mM (pH 5.5), 296K. The protein concentration in the relaxation experiments and at the beginning of the titrations was 1.5×10^{-3} M. The samples were left for 15 min at each GdmCl concentration before registering the corresponding measurement.

Atomic absorption

Quantitative analysis of copper in unfolded Rc was performed using a SpectraA-220FS (Varian) atomic absorption spectrometer equipped with an automated sampling system. Two Rc samples were metallated: One of them was oxidized and the other reduced. Excess metal and EDTA was eliminated from both as described above. Then, they were incubated with 6 M GdmCl for 1 h and dialyzed three times against the same buffer (3 h each). The final protein concentration of these samples was 7.0 μM. Atomic absorption spectroscopy was carried out with these two samples. The absorbance versus concentration (μg/L) calibration curve was previously determined following standard procedures.

NMR measurements

NMR experiments were performed at 296K in a Bruker Avance 500 spectrometer operating in a magnetic field of 11.7 Tesla. ^{1}H and ^{15}N frequencies were 500.13 and 50.68 MHz, respectively. The assignments of the peaks at a concentration of GdmCl of 2.1 M were achieved by following the chemical shifts from the native protein up to the incipient unfolded state present at that concentration of denaturant agent. A 3D ^{1}H-^{15}N HSQC-NOESY experiment (80 msec of mixing time) and a 3D ^{1}H-^{15}N HSQC-TOCSY (with 50 msec of spin lock) were also performed to assign some peaks in the most overcrowded regions. The carrier signal was set to the H_2O signal in all the experiments.

The unfolding process was monitored by NMR. ^{1}H-^{15}N HSQC experiments (Bodenhausen and Ruben 1980) were recorded after addition of the corresponding aliquots of a solution of 8.0 M GdmCl to the Rc sample. For the oxidized protein, a superweft ^{1}H experiment (Inubushi and Becker 1983) was also recorded at each point. In the first steps of the titrations an incipient unfolded state appears in fast exchange regime. Thus, the weighted average of the ^{1}H and ^{15}N chemical shifts can be calculated from the equation (Garrett et al. 1997):

$$\Delta\delta_{av} = \left[\left(\Delta\delta_{HN}^2 + (\Delta\delta_N/5)^2\right)/2\right]^{1/2} \quad (1)$$

where the differences $\Delta\delta_{HN}$ and $\Delta\delta_N$ refer to changes in the chemical shifts of the amide protons and the nitrogen atoms, respectively, between the incipient unfolded and completely folded species.

For higher concentrations of the denaturant agent, the incipient unfolded and completely unfolded species appear in a slow exchange regime. The molar fractions of both species, χ_F and χ_U, were determined from the ratios V_F/V_0 and V_U/V_0, respectively. Here, V_0 is the volume of the signal analyzed at the initial point of the titration (GdmCl 0.0 M) and V_F and V_U are the measured volumes of the cross peaks (corrected by the dilution factors) of the incipient and completely unfolded species, respectively.

The molar fraction of the aggregated species, χ_A (see Discussion) was calculated from the expression:

$$\chi_0 = \chi_F + \chi_U + \chi_A \quad (2)$$

where the total molar fraction, χ_0, equals unity.

For the H_2O/D_2O exchange experiments, a sample of GdmCl was lyophilized in D_2O. This deuterated GdmCl was used to prepare a stock solution of 2.1 M GdmCl in D_2O. A sample of Rc, previously lyophilized, was dissolved in the GdmCl solution and immediately introduced in an NMR tube. Then, a ^{1}H-^{15}N HSQC spectrum of this freshly prepared sample was recorded (0 h). HSQC experiments in analogous conditions were recorded every 15 min for the first 8 h, every 2 h the following 2 d, and at increasing intervals over 2 wk.

The decay of the individual peak volume was fitted to the single exponential decay curve, $I(t) = I(0)\ exp(R_{exch}t)$, where $I(t)$ and $I(0)$ are the volumes at a given time t and $t = 0$, respectively, and R_{exch} is the rate constant of the H_2O/D_2O exchange reaction. The protection factors, P, were calculated as $logP = log(R_{int}/R_{exch})$, where R_{int} is the intrinsic exchange rate for the proton (Hvidt and Nielsen 1966). In turn, R_{int} rates were calculated using the program SPHERE (http://www.fccc.edu/research/labs/roder/sphere).

Experiments to determine amide proton in exchange with the bulk solvent, ^{15}N-(CLEANEX-PM)-FHSQC (cleanex experiment) (Hwang et al. 1998), and with water molecules residing in the protein for longer than the correlation time (ePHOGSY) (Dalvit and Hommel 1995; Dalvit 1996) were also performed in a reduced sample (2.1 M GdmCl, acetate buffer 100 mM [pH 5.5]) by applying the previously reported pulse sequences.

The dynamic features of Rc in the reduced state in the presence of GdmCl 2.1 M were investigated by means of heteronuclear NMR. ^{15}N longitudinal, R_1 (Peng and Wagner 1994), and transversal, R_2 (Kay et al. 1992; Peng and Wagner 1994) relaxation rates, and the ^{1}H-^{15}N NOE (Grzesiek and Bax 1993) values were measured using the pulse sequences previously reported. For R_1 measurements, eight experiments with ^{15}N recovery delays of 10, 60, 130, 150, 250, 290, 500, and 800 msec were performed. The relaxation delay after the acquisition time was 3 sec. Another eight experiments with ^{15}N recovery delays of 6.9, 13.8, 27.6, 48.3, 75.9, 110.4, 151.8, and 207 msec during the transversal evolution of the ^{15}N nucleus were carried out to determine the R_2 values. Water suppression was achieved by an echo–anti-echo scheme (Sklenar and Bax 1987). For the determination of ^{1}H-^{15}N NOE values, three experiments with ^{1}H presaturation for 2.5 sec and one without were performed. In this last case, the strong solvent signal was partially eliminated by a flip-back approach (Grzesiek and Bax 1993). For R_2 and ^{1}H-^{15}N NOE experiments, 3.2 sec of recycle time were employed to ensure the complete relaxation of the nuclei.

For all NMR experiments, FIDs were apodized to a final data matrix of 2048×1024 points, zero filled, weighted by Gaussian and sine square functions (shifted 60°) in acquisition and evolution dimensions, respectively, and Fourier transformed. Only the downfield part of the ^{1}H spectra, containing the HN connectivities, was kept for the data analysis. All the NMR spectra were processed with the XWINNMR program (Bruker) and examined with the Sparky software (http://www.cgl.ucsf.edu/home/sparky/).

The mobility data were analyzed as previously described (Jiménez et al. 2003a, 2004). The overall tumbling of Rc was calculated from the R_2/R_1 ratios of each HN pair using the program Quadric Diffusion 1.11 (Lee et al. 1997). The average structure (previously minimized) of the family of Rc structures (1cur file [Botuyan et al. 1996] from the Protein Data Bank) was used in these calculations. R_2/R_1 values larger than twice the standard deviation (σ) of the average value were eliminated (Tjandra et al. 1995). This process was repeated until all values fell within the average value $\pm 2\sigma$. Throughout this article the same criterion has been taken for discerning between data that do and do not deviate from the average value. Relaxation rates that deviate $> 2\sigma$ are considered to deviate significantly from the average. The diffusion parameters corresponding to the isotropic, axially symmetric, and fully anisotropic models were tested (Palmer et al. 1991; Mandel et al. 1995). The F factor (Bevington and Robinson 1992) was used to check the statistical improvement of the fitting to each model.

The relaxation data (R_1, R_2, and ^{1}H-^{15}N NOE) were analyzed according to the model-free approach of Lipari and Szabo (1982a,b), using the program Modelfree 4.0 (Mandel et al. 1995). The experimental data were adjusted to one of the four different models described (Palmer et al. 1991; Mandel et al. 1995). Here, we follow exactly the same criteria as those previously reported (Jiménez et al. 2004).

Acknowledgments

This work has been supported with financial aid from the DGICYT-Ministerio de Ciencia y Tecnología, Spain (project nos. BQU2002–02236 and EET2002–05145). B.J. thanks the European Union Research and Training Network for a grant (Network "NMR Cross Correlation Rates as an avenue to study Biomolecules" n°HPRN-CT-2000–00092). The European Large Scale Facility PARABIO at the University of Florence, Italy (contract no. HPRI-CT-1999–00009) is acknowledged.

References

Alcaraz, L.A. and Donaire, A. 2004. Unfolding process of rusticyanin: Evidence of protein aggregation. *Eur. J. Biochem.* **271:** 4284–4292.

Bai, Y., Chung, J., Dyson, H.J., and Wright, P.E. 2001. Structural and dynamic characterization of an unfolded state of poplar apo-plastocyanin formed under nondenaturing conditions. *Protein Sci.* **10:** 1056–1066.

Banci, L., Bertini, I., Cramaro, F., Del Conte, R., Rosato, A., and Viezzoli, M.S. 2000. Backbone dynamics of human Cu,Zn superoxide dismutase and of its monomeric F50E/G51E/E133Q mutant: The influence of dimerization on mobility and function. *Biochemistry* **39:** 9108–9118.

Bertini, I., Dalvit, C., Luchinat, C., Huber, J.G., and Piccioli, M. 1997. e-PHOGSY experiments on a paramagnetic protein: Location of the catalytic water molecule in the heme crevice of the oxidized form of horse heart cytochrome *c*. *FEBS Lett.* **415:** 45–48.

Bertini, I., Bryant, D.A., Ciurli, S., Dikiy, A., Fernandez, C.O., Luchinat, C., Safarov, N., Vila, A.J., and Zhao, J. 2001a. Backbone dynamics of plastocyanin in both oxidation states. Solution structure of the reduced form and comparison with the oxidized state. *J. Biol. Chem.* **276:** 47217–47226.

Bertini, I., Luchinat, C., and Parigi, G. 2001b. *Solution NMR of paramagnetic molecules. Applications to metallobiomolecules and models. Current methods in inorganic chemistry*. Elsevier, Amsterdam.

Bevington, P.R. and Robinson, D.K. 1992. *Data reduction and error analysis for the physical sciences*, pp. 205–209. McGraw-Hill, New York.

Bodenhausen, G. and Ruben, D.J. 1980. Natural abundance nitrogen-15 NMR by enhanced heteronuclear spectroscopy. *Chem. Phys. Lett.* **69:** 185–189.

Botuyan, M.A., Toy-Palmer, A., Chung, J., Blake 2d, R.C., Beroza, P., Case, D.A., and Dyson, H.J. 1996. NMR solution structure of Cu(I) rusticyanin from *Thiobacillus ferrooxidans*: Structural basis for the extreme acid stability and redox potential. *J. Mol. Biol.* **263:** 752–767.

Bruschweiler, R. 2003. New approaches to the dynamic interpretation and prediction of NMR relaxation data from proteins. *Curr. Opin. Struct. Biol.* **13:** 175–183.

Buning, C., Canters, G.W., Comba, P., Dennison, C., Jeuken, L., Melter, M., and Sanders-Loehr, J. 2000. Loop-directed mutagenesis of the blue copper protein amicyanin from *Paracoccus versutus* and its effect on the structure and the activity of the type-1 copper site. *J. Am. Chem. Soc.* **122:** 204–211.

Campos-Olivas, R. and Summers, M.F. 1999. Backbone dynamics of the N-terminal domain of the HIV-1 capsid protein and comparison with the G94D mutant conferring cyclosporin resistance/dependence. *Biochemistry* **38:** 10262–10271.

Capaldi, A.P., Ferguson, S.J., and Radford, S.E. 1999. The Greek key protein apo-pseudoazurin folds through an obligate on-pathway intermediate. *J. Mol. Biol.* **286:** 1621–1632.

Cox, J.C. and Boxer, D.H. 1978. The purification and some properties of rusticyanin, a blue copper protein involved in iron(II) oxidation from *Thiobacillus ferro-oxidans*. *Biochem. J.* **174:** 497–502.

Crane, B.R., Di Bilio, A.J., Winkler, J.R., and Gray, H.B. 2001. Electron tunneling in single crystals of *Pseudomonas aeruginosa* azurins. *J. Am. Chem. Soc.* **123:** 11623–11631.

Daggett, V. and Fersht, A.R. 2003. Is there a unifying mechanism for protein folding? *Trends Biochem. Sci.* **28:** 18–25.

Dalvit, C. 1996. Homonuclear 1D and 2D NMR experiments for the observation of solvent-solute interactions. *J. Magn. Reson. B* **112:** 282–288.

Dalvit, C. and Hommel, U. 1995. Sensitivity-improved detection of protein hydration and its extension to the assignment of fast-exchanging resonances. *J. Magn. Reson. B* **109:** 334–338.

Dinner, A.R., Sali, A., Smith, L.J., Dobson, C.M., and Karplus, M. 2000. Understanding protein folding via free-energy surfaces from theory and experiment. *Trends Biochem. Sci.* **25:** 331–339.

Dobson, C.M. 2003. Protein folding and misfolding. *Nature* **426:** 884–890.

Donaire, A., Jiménez, B., Moratal, J.M., Hall, J.F., and Hasnain, S.S. 2001. Electronic characterization of the oxidized state of the blue copper protein rusticyanin by ^{1}H NMR: Is the axial methionine the dominant influence for the high redox potential? *Biochemistry* **40:** 837–846.

Donaire, A., Jimenez, B., Fernandez, C.O., Pierattelli, R., Niizeki, T., Moratal, J.M., Hall, J.F., Kohzuma, T., Hasnain, S.S., and Vila, A.J. 2002. Metal-ligand interplay in blue copper proteins studied by ^{1}H NMR spectroscopy: Cu(II)-pseudoazurin and Cu(II)-rusticyanin. *J. Am. Chem. Soc.* **124:** 13698–13708.

Dyson, H.J. and Wright, P.E. 2002. Insights into the structure and dynamics of unfolded proteins from nuclear magnetic resonance. *Adv. Protein Chem.* **62:** 311–340.

Dyson, H.J., Merutka, G., Waltho, J.P., Lerner, R.A., and Wright, P.E. 1992. Folding of peptide fragments comprising the complete sequence of proteins. Models for initiation of protein folding. I. Myohemerythrin. *J. Mol. Biol.* **226:** 795–817.

Ferguson, N. and Fersht, A.R. 2003. Early events in protein folding. *Curr. Opin. Struct. Biol.* **13:** 75–81.

Fersht, A.R. and Daggett, V. 2002. Protein folding and unfolding at atomic resolution. *Cell* **108:** 573–582.

Garrett, D.S., Seok, Y.J., Peterkofsky, A., Clore, G.M., and Gronenborn, A.M. 1997. Identification by NMR of the binding surface for the histidine-containing phosphocarrier protein HPr on the N-terminal domain of enzyme I of the *Escherichia coli* phosphotransferase system. *Biochemistry* **36:** 4393–4398.

Gianni, S., Guydosh, N.R., Khan, F., Caldas, T.D., Mayor, U., White, G.W., DeMarco, M.L., Daggett, V., and Fersht, A.R. 2003. Unifying features in protein-folding mechanisms. *Proc. Natl. Acad. Sci.* **100:** 13286–13291.

Gray, H.B., Malmström, B.G., and Williams, R.J.P. 2000. Copper coordination in blue proteins. *J. Biol. Inorg. Chem.* **5:** 551–559.

Grzesiek, S. and Bax, A. 1993. The importance of not saturating water in protein NMR. Application to sensitivity enhancement and NOE measurements. *J. Am. Chem. Soc.* **115:** 12593–12594.

Hall, J.F., Hasnain, S.S., and Ingledew, W.J. 1996. The structural gene for rusticyanin from *Thiobacillus ferrooxidans:* Cloning and sequencing of the rusticyanin gene. *FEMS Microbiol. Lett.* **137:** 85–89.

Hvidt, A. and Nielsen, S.O. 1966. Hydrogen exchange in proteins. *Adv. Protein Chem.* **21:** 287–386.

Hwang, T.-L., van Zijl, P.C.M., and Mori, S. 1998. Accurate quantitation of water-amide proton exchange rates using the phase-modulated CLEAN chemical EXchange (CLEANEX-PM) approach with a Fast-HSQC (FHSQC) detection exchange. *J. Biomol. NMR* **11:** 221–226.

Ingledew, W.J. and Cobley, J.G. 1980. A potentiometric and kinetic study on the respiratory chain of ferrous-iron-grown *Thiobacillus ferrooxidans*. *Biochim. Biophys. Acta* **590:** 141–158.

Inubushi, T. and Becker, E.D. 1983. Efficient detection of paramagnetically shifted NMR resonances by optimizing the WEFT pulse sequence. *J. Magn. Reson.* **51:** 128–133.

Jiménez, B., Piccioli, M., Moratal, J.M., and Donaire, A. 2003a. Backbone dynamics of rusticyanin: The high hydrophobicity and rigidity of this blue copper protein is responsible for its thermodynamic properties. *Biochemistry* **42:** 10396–10405.

Jiménez, B., Poggi, L., and Piccioli, M. 2003b. Monitoring the early steps of unfolding of dicalcium and mono-Ce3 + -substituted forms of P43M calbindin D9k. *Biochemistry* **42:** 13066–13073.

Jiménez, B., Moratal, J.M., Piccioli, M., and Donaire, A. 2004. Mobility studies in proteins by ^{15}N nuclear magnetic resonance: Rusticyanin as an example. In *Methods in proteome and protein analysis* (eds. R.M. Kamp et al.), pp. 15–33. Springer, Berlin.

Kalverda, A.P., Ubbink, M., Gilardi, G., Wijmenga, S.S., Crawford, A., Jeuken, L.J., and Canters, G.W. 1999. Backbone dynamics of azurin in solution: Slow conformational change associated with deprotonation of histidine 35. *Biochemistry* **38:** 12690–12697.

Kay, L.E., Nicholson, L.K., Delaglio, F., Bax, A., and Torchia, D.A. 1992. Pulse sequences for removal of the effects of cross correlation between dipolar and chemical-shift anisotropyrelaxation mechanisms on the measurement of heteronuclear T1 and T2 values in proteins. *J. Magn. Reson.* **97:** 359–375.

Kjellsson, A., Sethson, I., and Jonsson, B.H. 2003. Hydrogen exchange in a large 29 kD protein and characterization of molten globule aggregation by NMR. *Biochemistry* **42:** 363–374.

Kobayashi, T., Ikeguchi, M., and Sugai, S. 2000. Molten globule structure of equine β-lactoglobulin probed by hydrogen exchange. *J. Mol. Biol.* **299:** 757–770.

Leckner, J., Bonander, N., Wittung-Stafshede, P., Malmstrom, B.G., and Karlsson, B.G. 1997a. The effect of the metal ion on the folding energetics of azurin: A comparison of the native, zinc and apoprotein. *Biochim. Biophys. Acta* **1342:** 19–27.

Leckner, J., Wittung, P., Bonander, N., Karlsson, B.G., and Malmström, B.G. 1997b. The effect of redox state on the folding free energy of azurin. *J. Biol. Inorg. Chem.* **2:** 368–371.

Lee, L.K., Rance, M., Chazin, W.J., and Palmer, A.G. 1997. Rotational diffusion anisotropy of proteins from simultaneous analysis of ^{15}N and ^{13}C α nuclear spin relaxation. *J. Biomol. NMR* **9:** 287–298.

Li, H., Webb, S.P., Ivanic, J., and Jensen, J.H. 2004. Determinants of the relative reduction potentials of type-1 copper sites in proteins. *J. Am. Chem. Soc.* **126:** 8010–8019.

Lipari, G. and Szabo, A. 1982a. Model-free approach to the interpretation of nuclear magnetic resonance relaxation in macromolecules. 1. Analysis of experimental results. *J. Am. Chem. Soc.* **104:** 4559–4570.

———. 1982b. Model-free approach to the interpretation of nuclear magnetic resonance relaxation in macromolecules. 1. Theory and range of validity. *J. Am. Chem. Soc.* **104:** 4546–4559.

Malmström, B.G. 1964. Two forms of copper in copper-containing oxidases. In *Oxidases and related redox systems* (eds. T.E. King et al.), pp. 207–216. Wiley, New York.

———. 1994. Rack-induced bonding in blue-copper proteins. *Eur. J. Biochem.* **233:** 711–718.

Malmstrom, B.G. and Leckner, J. 1998. The chemical biology of copper. *Curr. Opin. Chem. Biol.* **2:** 286–292.

Mandel, A.M., Akke, M., and Palmer, A.G. 1995. Backbone dynamics of *Escherichia coli* ribonuclease HI: Correlations with the structure and function in an active enzyme. *J. Mol. Biol.* **246:** 144–163.

Marks, J., Pozdnyakova, I., Guidry, J., and Wittung-Stafshede, P. 2004. Methionine-121 coordination determines metal specificity in unfolded *Pseudomonas aeruginosa* azurin. *J. Biol. Inorg. Chem.* **9:** 281–288.

Mizuguchi, M., Kroon, G.J., Wright, P.E., and Dyson, H.J. 2003. Folding of a β-sheet protein monitored by real-time NMR spectroscopy. *J. Mol. Biol.* **328:** 1161–1171.

Nunzi, F., Guerlesquin, F., Shepard, W., Guigliarelli, B., and Bruschi, M. 1994. Active site geometry in the high oxido-reduction potential rusticyanin from *Thiobacillus ferrooxidans*. *Biochem. Biophys. Res. Commun.* **203:** 1655–1662.

O'Halloran, T.V. and Culotta, V.C. 2000. Metallochaperones, an intracellular shuttle service for metal ions. *J. Biol. Chem.* **275:** 25057–25060.

Olsson, M.H., Hong, G., and Warshel, A. 2003. Frozen density functional free energy simulations of redox proteins: Computational studies of the reduction potential of plastocyanin and rusticyanin. *J. Am. Chem. Soc.* **125:** 5025–5039.

Palmer 3d, A.G., Rance, M., and Wright, J.G. 1991. Intramolecular motions of a zinc finger DNA-binding domain from Xfin characterized by proton-detected natural abundance carbon-13 heteronuclear NMR spectroscopy. *J. Am. Chem. Soc.* **113:** 4371–4380.

Peng, J.W. and Wagner, G. 1994. Investigation of protein motions via relaxation measurements. *Methods Enzymol.* **239:** 563–596.

Pozdnyakova, I. and Wittung-Stafshede, P. 2001a. Biological relevance of metal binding before protein folding. *J. Am. Chem. Soc.* **123:** 10135–10136.

———. 2001b. Copper binding before polypeptide folding speeds up formation of active (holo) *Pseudomonas aeruginosa* azurin. *Biochemistry* **40:** 13728–13733.

———. 2002. If space is provided, bulky modification on the rim of azurin's β-barrel results in folded protein. *FEBS Lett.* **531:** 209–214.

———. 2003. Approaching the speed limit for Greek Key β-barrel formation: Transition-state movement tunes folding rate of zinc-substituted azurin. *Biochim. Biophys. Acta* **1651:** 1–4.

Pozdnyakova, I., Guidry, J., and Wittung-Stafshede, P. 2001. Probing copper ligands in denatured *Pseudomonas aeruginosa* azurin: Unfolding His117Gly and His46Gly mutants. *J. Biol. Inorg. Chem.* **6:** 182–188.

Randall, D.W., Gamelin, D.R., LaCroix, L.B., and Solomon, E.I. 2000. Electronic structure contributions to electron transfer in blue Cu and CuA. *J. Biol. Inorg. Chem.* **5:** 16–19.

Romero, C., Moratal, J.M., and Donaire, A. 1998. Metal coordination of azurin in the unfolded state. *FEBS Lett.* **440:** 93–98.

Sandberg, A., Harrison, D.J., and Karlsson, B.G. 2003. Thermal denaturation of spinach plastocyanin: Effect of copper site oxidation state and molecular oxygen. *Biochemistry* **42:** 10301–10310.

Schwalbe, H. 2003. Kurt Wuthrich, the ETH Zurich, and the development of NMR spectroscopy for the investigation of structure, dynamics, and folding of proteins. *Chembiochem* **4:** 135–142.

Sklenar, V. and Bax, A. 1987. Spin-echo water suppression for the generation of pure-phase two-dimensional NMR spectra. *J. Magn. Reson.* **74:** 469–479.

Thompson, G.S., Leung, Y.C., Ferguson, S.J., Radford, S.E., and Redfield, C. 2000. The structure and dynamics in solution of Cu(I) pseudoazurin from *Paracoccus pantotrophus*. *Protein Sci.* **9:** 846–858.

Tjandra, N., Kuboniwa, H., Ren, H., and Bax, A. 1995. Rotational dynamics of calcium-free calmodulin studied by ^{15}N-NMR relaxation measurements. *Eur. J. Biochem.* **230:** 1014–1024.

Vendruscolo, M., Paci, E., Karplus, M., and Dobson, C.M. 2003. Structures and relative free energies of partially folded states of proteins. *Proc. Natl. Acad. Sci.* **100:** 14817–14821.

Vila, A.J. and Fernandez, C.O. 2001. Copper in electron-transfer proteins. In *Handbook on metalloproteins* (eds. I. Bertini and H. Sigel), pp. 813–856. Marcel Dekker, New York.

Walter, R.L., Ealick, S.E., Friedman, A.M., Blake 2d, R.C., Proctor, P., and Shoham, M. 1996. Multiple wavelength anomalous diffraction (MAD) crystal structure of rusticyanin: A highly oxidizing cupredoxin with extreme acid stability. *J. Mol. Biol.* **263:** 730–751.

Winkler, J.R., Wittung-Stafshede, P., Leckner, J., Malmstrom, B.G., and Gray, H.B. 1997. Effects of folding on metalloprotein active sites. *Proc. Natl. Acad. Sci.* **94:** 4246–4249.

Wittung-Stafshede, P. 2004. Role of cofactors in folding of the blue-copper protein azurin. *Inorg. Chem.* **43:** 7926–7933.

Wittung-Stafshede, P., Hill, M.G., Gomez, E., Di Bilio, A.J., Karlson, B.G., Leckner, J., Winkler, J.R., Gray, H.B., and Malmstrom, B. 1998. Reduction potentials of blue and purple copper proteins in their unfolded states: A closer look at rack-induced coordination. *J. Biol. Inorg. Chem.* **3:** 367–370.